Regular article

Sea surface temperature inversion model for infrared remote sensing images based on deep neural network

Bo Ai[a], Zhen Wen[a], Yingchao Jiang[a], Song Gao[b,*], Guannan Lv[a,c]

[a] College of Geomatics, Shandong University of Science and Technology, Qingdao 266590, China
[b] North China Sea Marine Forecasting Center of State Oceanic Administration, Qingdao 266061, China
[c] Qingdao Yuehai Information Service Co., Ltd., Qingdao 266590, China

ABSTRACT

The traditional sea surface temperature (SST) inversion model has a complicated parameter fitting process and poor adaptability in different sea areas. This paper presents an infrared remote sensing inversion model of SST based on deep neural network to refine the situation. The training data are the moderate-resolution imaging spectroradiometer (MODIS) infrared remote sensing data on sunny days and measured data from buoy in Bohai. The accuracy of inversion results is analyzed, the determination coefficient of inversion and measured values is 0.98, the standard error is 0.71 °C and the mean absolute deviation is 0.85 °C, the results show good accuracy of the model. The accuracy of Bohai SST inversion results is compared with SST products from the MODIS sensors and the inversion model is applied to other sea areas, demonstrating the credibility and portability of the model. The data experiments in this paper prove the feasibility of the model, which provides ideas for global SST inversion.

1. Introduction

Sea surface temperature (SST) is one of the physical parameters of ocean. It plays an important role in the research and engineering of oceans, meteorology and fisheries. The SST observation data obtained by traditional ships and buoys is discontinuous in time and space. Therefore, infrared remote sensing data has become an important data source for SST inversion due to its wide coverage of time and space and high spatial resolution [1].

Many domestic and foreign scholars have carried out research on SST inversion using infrared remote sensing methods, and the most widespread approach is the linear regression statistical model based on split window technology [2]. McClain et al. [3] first proposed the SST inversion method - multi-channel sea surface temperature (MCSST) inversion method based on Advanced Very High Resolution Radiometer (AVHRR) thermal infrared image and inverted the global temperature data of 4 km spatial resolution. Zhu et al. [4] researched SST inversion in the East China Sea employing the 20, 29, 31 and 32 infrared channel data of MODIS, and simulated algorithm coefficient by atmospheric radiation transmission, the SST distribution obtained in this way is consistent with the MOD28 production. Liu et al. [5] put forward the multi-channel split window algorithm to invert the SST in the Yellow Sea and the East Sea, which reflected the SST distribution more

realistically. Current calculation method for parameter fitting of linear statistical regression model used in SST inversion research is complicated and cumbersome. In addition, simple linear regression often cannot express the complex relationship between sea temperature factors. Thus, this limitation results in low adaptability in different sea areas.

Deep learning is a new field in machine learning research, which establishes neural network simulating human brain to analyze and imitate the mechanism of human brain to interpret data. It has been widely used in image and speech recognition [6]. In the field of remote sensing, Xu [7] used deep neural network (DNN) model in deep learning to invert sea surface salinity and obtained satisfying results, Shi et al. [8] proposed a fast pixel-wise labeling method called scanning convolutional network (SCN) for mudflat aquaculture area detection with infrared remote sensing images, Kim et al. [9] described a new approach to near-future prediction of Arctic sea ice concentration (SIC) by employing a deep learning method with multi-model ensemble, which showed a broader application of deep learning in remote sensing.

This paper presents a DNN model for remote sensing inversion of SST to solve complex parameter fitting and poor adaptability in traditional sea temperature inversion model. The model with a simple and accurate calculation process better fits the nonlinear relationship between remote sensing parameters and SST. Based on the MCSST

inversion method, this paper comprehensively considers various influencing factors, selects remote sensing parameters closely related to SST, and preprocesses remote sensing data according to the selected parameters to establish a DNN model with multiple hidden layers. The accuracy analysis of the inversion results is carried out, and the reasons that affect the accuracy of the inversion model are explained in this paper.

2. Deep learning inversion method

Neural network is the key technology in deep learning [10]. Its operational principle is as follows. First, the signals of input parameters are propagated forward according to the connection weight between initialized neurons. Second, the errors are propagated backward according to the backpropagation (BP) algorithm after reaching the output layer. Finally, the weight and error of the network connection are adjusted by the gradient descent method to reduce the error. Thus, network's output value is close to the expected value. There are multiple hidden layers in deep neural networks than ordinary neural networks, which means that deep neural networks have stronger data fitting ability. The essence of deep learning is to achieve a precise representation for complex nonlinear functions between input features and output results by establishing a DNN with multiple hidden layers and repeatedly fitting training data [11].

This paper proposes a deep learning inversion model, its general idea is as follows. First, the input parameters of the model are determined, the image data is preprocessed, and the inversion data set that corresponds to SST is obtained. Then, the model that maps input data to output variable is determined, and the data is randomly sorted and incorporated into the SST inversion model based on DNN. Finally, the inversion results are verified in accuracy according to a part of the measured sea temperature, and the model parameters are adjusted to determine the optimal inversion model with the best accuracy. The specific technical procedures are shown in Fig. 1.

The input elements of the inversion model should be determined by selecting remote sensing parameters before establishing and training the model. These elements are selected according to the relevant remote sensing parameters in the MCSST inversion method. The algorithm formula is Eq. (1) [3]:

$$T_s = C_1 + C_2 \times T_i + C_3 \times (T_i - T_j) + f \tag{1}$$

In this formula, T_i and T_j are the brightness temperatures of any two thermal infrared bands in the MODIS satellite sensor, f is the influence error caused by other variables (such as instantaneous zenith angle θ of satellite sensors), C_1, C_2 and C_3 are model coefficients. The 31-band and 32-band brightness temperature are selected because the two adjacent thermal infrared bands in the MODIS remote sensing data are universally applied to temperature inversion. The deep neural network mainly establishes a connection between the input parameters and the output parameters. The correlation between the input parameters and the output parameters is higher, the effect is better [12]. Therefore, the focus is to eliminate the influence of other factors on the input parameters. The difference between the brightness temperature of the two thermal infrared channels, the instantaneous zenith angle of the satellite sensor and the atmospheric transmittance can respectively correct the effects of atmospheric weakening, thermal infrared radiation transmission path and atmospheric influence, which are shown in Table 1.

3. Data source and preprocessing

The data quality of the input elements has a significant impact on the accuracy of the deep learning model, so the data entered to the model should be preprocessed. The preprocessed data obtains the five remote sensing parameters determined above, the measured buoy data is filtered to match with the remote sensing data of the corresponding time and place to form a data set.

3.1. Data source

Bohai is an inland sea in China, which has abundant resources. However, the current marine environmental situation in the Bohai is particularly severe. Studying the changes in environmental factors in the Bohai area is an important issue. Bohai is selected as the research area in this paper. The data is composed of remote sensing image data and the measured SST buoy data. The data is uncloudy remote sensing data distributed evenly in the morning or afternoon each month from 2013 to 2016 including the MODIS L1B level 1KM resolution remote sensing image and MOD03 geographic coordinate data from the NASA LAADS Web for a total of 173 images [13]. The measured data is the SST buoy data of five stations in the Bohai Sea area corresponding to the time of remote sensing data provided by the North China Sea Branch of State Oceanic Administration. The position of the buoy is shown in Table 2 and Fig. 2.

3.2. Data preprocessing

3.2.1. Remote sensing data preprocessing

The preprocessing of the data is done by The Environment for Visualizing Images (ENVI), which is divided into the following steps. First, the data is read as Hierarchical Data Format (HDF) file and stored as Band Sequential (BSQ), and the brightness temperatures (T_{31} and T_{32}) of the 31-band and 32-band are estimated. Second, the radiance calibration is operated to obtain the radiance value of the 31-band and 32-band from the pixel gray value of the original image. The calculation formula Eq. (2) is derived according to the Planck function to get brightness temperature [14]. In this formula, K_{i1} and K_{i2} are constant, i is band number. For 31-band, $K_{31,1} = 729.541 \, \text{W/(m}^2 \, \text{sr} \, \text{µm)}$, $K_{31,2} = 1304.414 \, \text{K}$. For 32-band, $K_{32,1} = 474.685 \, \text{W/(m}^2 \, \text{sr} \, \text{µm)}$, $K_{32,2} = 1196.979 \, \text{K}$.

$$T_i = \frac{K_{i2}}{\ln(1 + \frac{K_{i1}}{I_i})} \tag{2}$$

Then, the processed data is subjected to automatic geometric correction for the reflectance data set and the 31, 32-band. Finally, the atmospheric transmissivity of the 31 and 32 bands are determined by the empirical formula Eq. (3) proposed by Mao et al. [15]. In the formula, $R2$ and $R19$ are the reflectivity of the 2 and 19 bands respectively.

$$\begin{cases} \tau_{31} = -0.124((0.02 - \ln(R_{19}/R_2))/0.651)^2 + 1.047 \\ \tau_{32} = -0.145((0.02 - \ln(R_{19}/R_2))/0.651)^2 + 0.997 \end{cases} \tag{3}$$

3.2.2. Measured data screening

The measured buoy data records SST by hour, while the satellite transit time only consists of two moments in a day, which includes ante meridiem time from Terra and post meridiem from Aqua. The measured buoy data needs to be filtered to match the satellite transit time in the experiment. There are two rules when screening measured data. First, if the time is not the integral point, take the nearest integral point. Second, if the data defaults in the measured buoy data, the data at the nearest moment is selected instead. There is almost no difference in SST between two times because sea temperature is a slowly mutative value. For instance, if the image time is three forty-five o'clock and the time four o'clock in measured data defaults, the three o'clock will be selected. 778 measured data corresponding to remote sensing data are selected for the SST inversion in this way.

4. Inversion model establishment

From the preprocessed MODIS satellite image, five remote sensing parameters T_{31}, T_{31}-T_{32}, θ, τ_{31} and τ_{32} corresponding to the measured
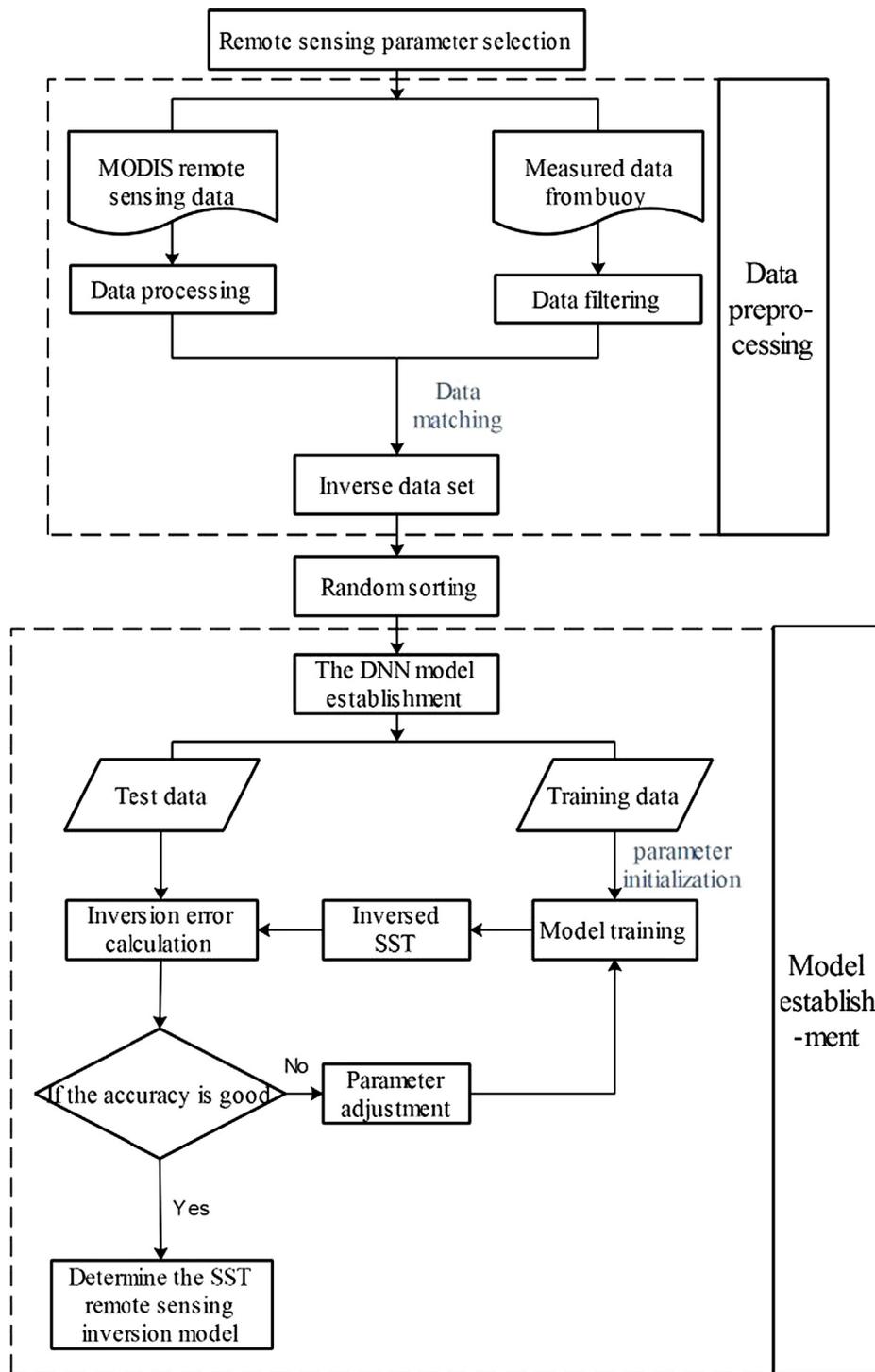
Fig. 1. Technology Procedures.

Table 1
Inversion Model Input Factor.

Remote sensing parameter	Meaning
T_{31}	The brightness temperature of band 31
T_{31}-T_{32}	The difference between the brightness temperature of band 31 and band 32
Sec(θ)	The satellite sensor's zenith
τ_{31}	The atmospheric transmittance of band 31
τ_{32}	The atmospheric transmittance of band 32

Table 2
The Measured Buoy Site in Bohai.

Number	Longitude (°E)	Latitude (°N)
1	120.5987	39.4995
2	120.0810	39.0227
3	121.1578	38.5495
4	121.0672	38.1583
5	119.8510	38.0330
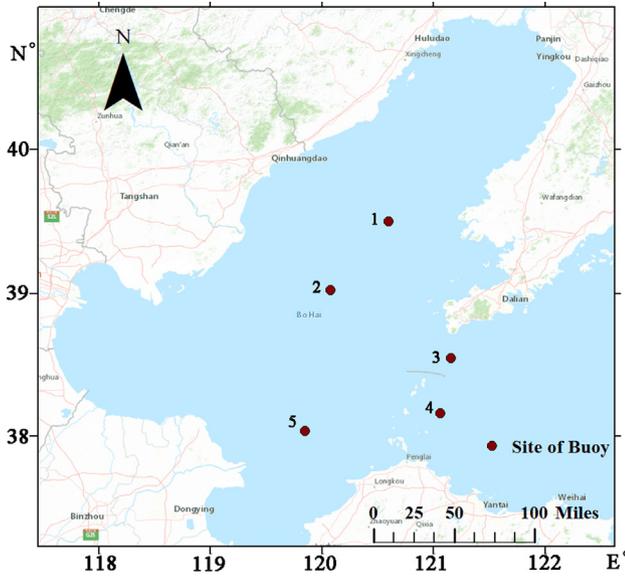
Fig. 2. The Measured Buoy Site Distribution in Bohai.

Table 3
Model parameter setting.

Parameter	Value
Number of input layer's node points	5
Number of hidden layers	4
Activation function	Relu
Optimization function	Admax
Number of Iterations	4400
Initial learning rate	0.001
Batch size	150

activation function of the layer, and the results spread forward layer by layer. In the model training, the BP algorithm is used to calculate the derivative of the loss function mean-square error (MSE) to optimize the weight and offset of each layer. The loss function Eq. (4) is as follows.

$$MSE = \sum_{i=1}^{N} (y_i - \hat{y}_i)^2 \tag{4}$$

where y_i is the inversion SST by the model, $\hat{y}_i$ is the measured SST, N is the total number of samples. The following Fig. 3 is the structure diagram of the DNN model. This neural network model has four hidden layers, the ellipses represent the input neurons, the circles represent the neurons in hidden layers, the rectangles represent the output neurons, the rhombuses represent the bias units and the values $W_{ij}^{(1)}$ on the connecting line indicates the connection weight between the i + 1th neuron in the first layer and the i + 1th neuron in the i + 1th layer.

4.2. Parameter optimization

In the process of model building and training, the optimization strategy for the selection and application of the activation function is as follows.

4.2.1. Model activation function selection

In DNN, the function relationships between input features and output targets are fitted by parameters and activation functions. Functions such as Sigmoid ($f(x) = (1 + e^{-x})^{-1}$)), Relu ($f(x) = \max (0,$
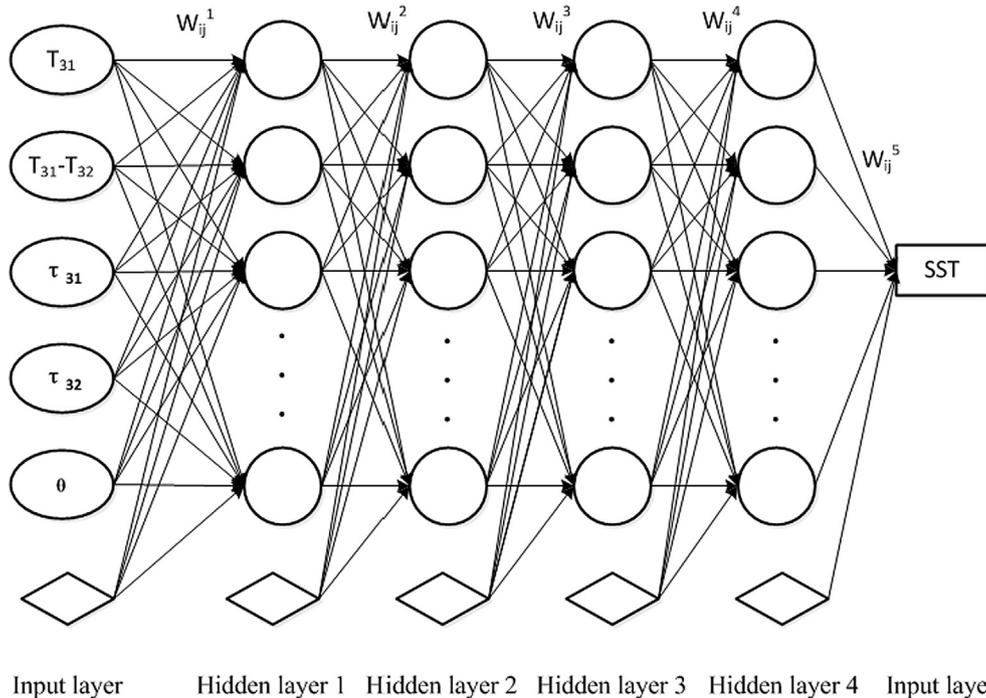
data are selected as input elements, and SST is used as the output variable. The 778 sets of data are composed of the remote sensing parameter data and the sea temperature measured buoy data. These data are randomly arranged and divided into training data and test data, the training data are 605 sets, and the test data are 173 sets for model training and SST inversion. The SST data set is ready for the model after these steps.

4.1. Model framework

The inversion model is a feedforward multi-layer perceptron model with one input layer, multiple hidden layers and one output layer. The input of the deep neural network is a vector composed of five remote sensing parameters. The output of the upper hidden layer is used as an input vector, the nonlinear conversion is performed according to the

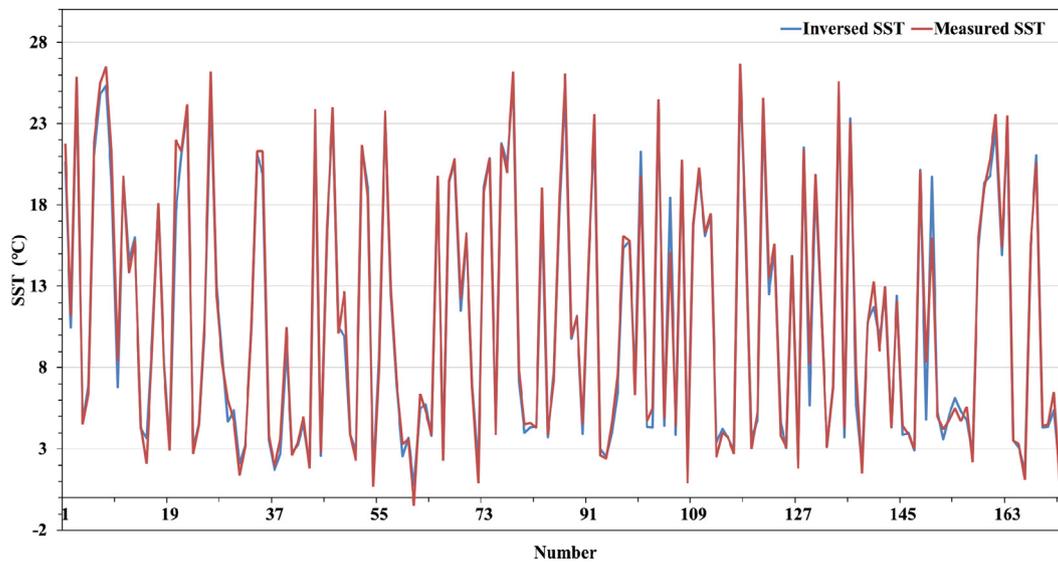

Fig. 3. DNN Model Structure.
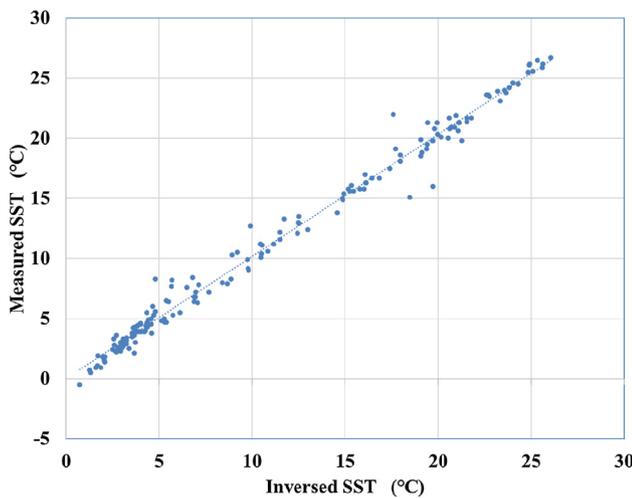
Fig. 4. Inversion Results.

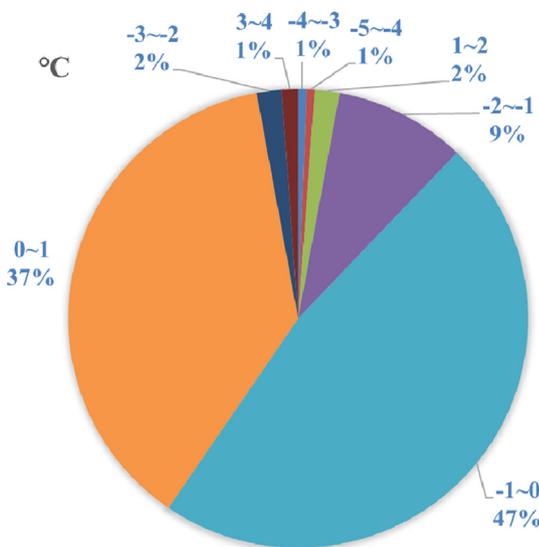**Fig. 5.** Measured and Inversed Regression Results.

Fig. 6. Error Statistics Pie Chart.

Table 4
Error Statistics of MODIS SST Inversion Model.

Author	The mean absolute error(˚C)	The standard error(˚C)	The maximum absolute error(˚C)
Song [22]	1.22	1.84	/
Lin [14]	/	1.75	/
Su [23]	1.38	1.77	4.98
This paper	0.85	0.71	4.05

x)) and Tanh ($f(x) = tanh\ (x)$) are used as activation functions of neurons. Relu is used as the activation function in this neural network. This function is different from the traditional nonlinear function. It is a piecewise linear function: when x is greater than 0, the output is equal to the input, when x is less than 0, the output is zero. Since the BP algorithm is used in the model training, the derivation of Sigmoid approaches to zero easily, known as gradient dispersion, which leads to the weight cannot be iterated. In addition, the derivation process of Sigmoid and Tanh is complicated, resulting in a decline in model efficiency [10]. Relu has a faster convergence speed than the traditional saturated nonlinear function when the training gradient declines, so the training speed is much faster than the traditional method when training the whole network [16]. The above three activation functions are respectively tried in the actual operation. The results show that the model converges fastest and performs best when the activation function is Relu. As a result, this paper selects Relu as the activation function considering the above factors and experimental situation.

4.2.2. Dropout algorithm

When the amount of data is small, the model is still prone to overfit due to the complex structure and numerous parameters in DNN. Dropout is a technique to prevent overfitting by preventing the complex correlation between training data [17]. It is selected to prevent overfitting and improve the generalization ability of the model. The principle of the algorithm is temporarily discarding the neurons from the network according to a certain probability during the training phase. Dropout is added to the DNN, the following formula Eq. (5) takes a certain neuron as an example.

$$O_i = X_i a\left(\sum_{k=1}^{d_i} w_k x_k + b \right) = \begin{cases} a(\sum_{k=1}^{d_i} w_k x_k + b) & X_i = 1 \\ 0 & X_i = 0 \end{cases} \tag{5}$$

where w_k and b are the weight and bias of the current neurons respectively, X_i is a random vector obeying the Bernoulli distribution and
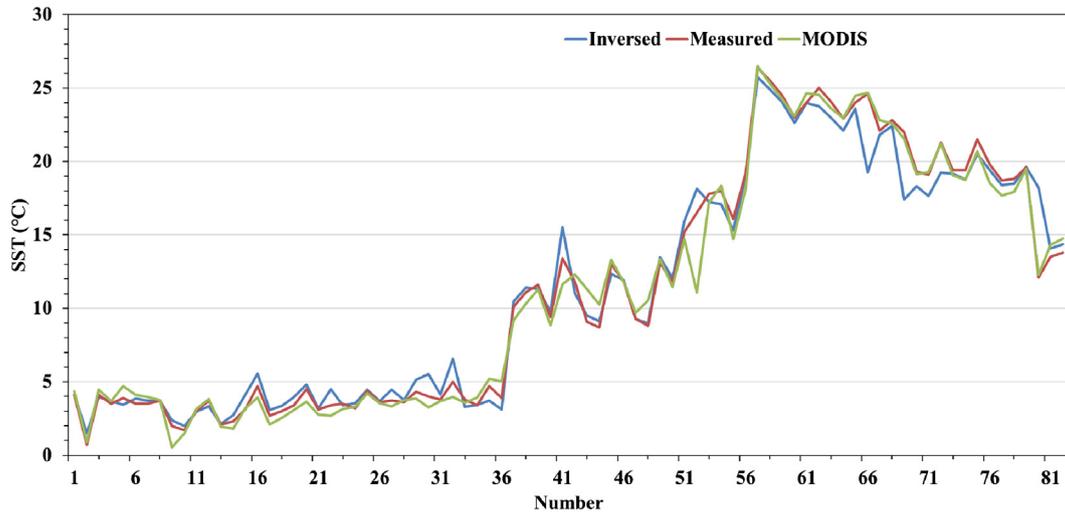
Fig. 7. Comparison of Three Types of SST Data.

Table 5
Error Statistics of Regional SST Inversion.

Fig. Number	Date	MSE	Mean Absolute Deviation
8-1	June 16	1.7	1.6
8-2	October 14	1.1	1.0
8-3	November 15	2.6	2.5

Table 6
The Measured Buoy Site in South China Sea.

Number	Longitude (°E)	Latitude (°N)
1	117.0993	21.8663
2	113.9992	21.5000
3	112.6330	21.1158

only containing 0 and 1. x_k is the input variable generated from the previous network layer, O_i is the activation value (output result) of the neurons, d_i is the number of neurons connected to neurons in the previous layer, $a(x)$ is the nonlinear activation function. According to Hinton's research, the model has good effect when the parameter value is 0.5.

4.2.3. Optimization function and learning rate setting

This paper chooses self-adaptation learning rate optimization method, Admax, to train the inversion model [18]. The method uses the first moment estimation and the second moment estimation of the gradient to dynamically adjust the learning rate of each parameter. The main advantage is that each iteration learning rate has a certain range after the offset correction, which makes the parameters relatively
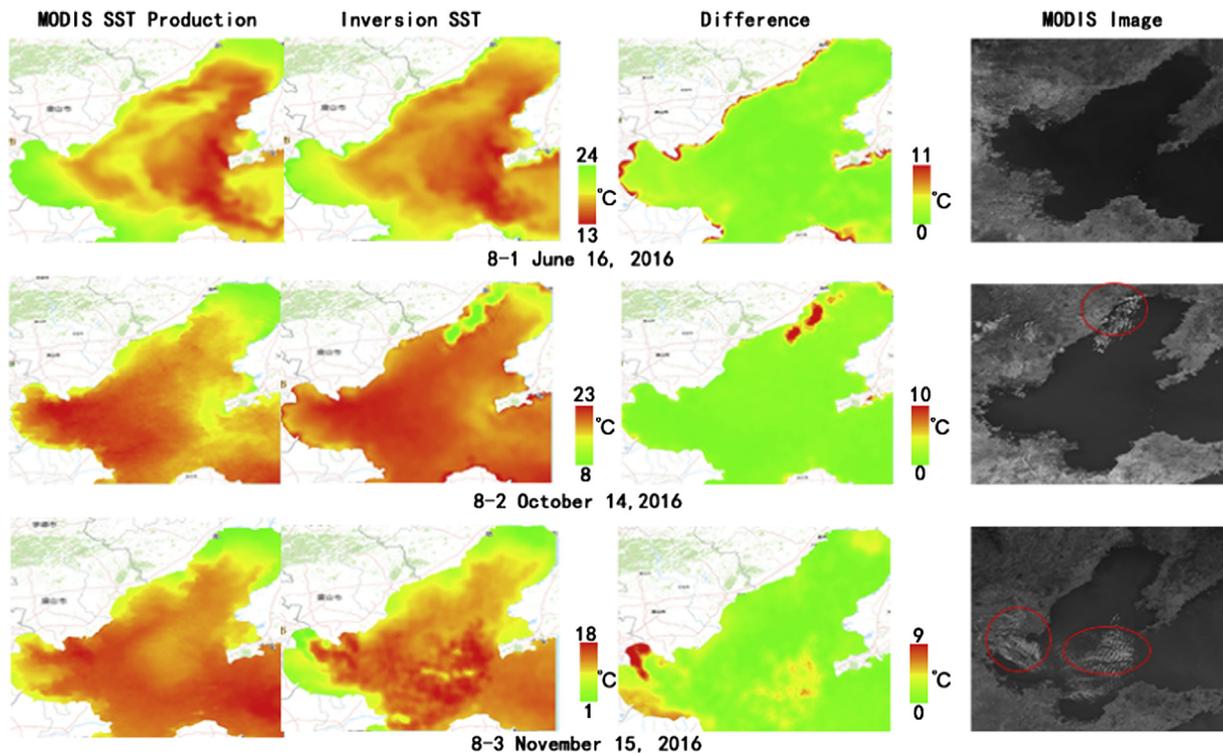
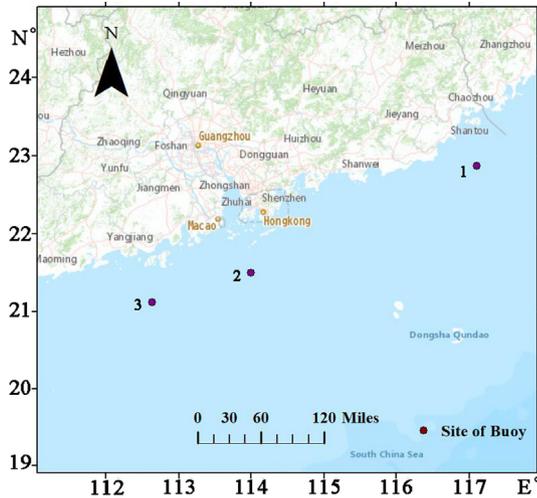

Fig. 8. Regional SST Inversion.

Fig. 9. The Measured Buoy Site Distribution in South China Sea.

stable. The learning rate has an important influence on the training efficiency of the model. The model will oscillate if the rate is too large, and the model will converge too slowly if the rate is too small. The model is trained by a progressively decaying learning rate. The initial learning rate is 0.002 in the training process. Observing the error of the test set until it is invariably, the learning rate is gradually attenuated by multiplying the multiplier factor with a value (0.5 or 0.2) as the number of iterations increases.

Since there are no uniform rules for the setting of model parameters at present, the model parameters are adjusted according to experience with continuously running the model. Finally, the specific structure of the inversion model is determined using python [19], neurons in the four hidden layers are 600, 500, 400, and 300 respectively. The optimal parameter configuration is shown in Table 3 [20].

5. Inversion model analysis

This section analyzes Bohai SST inversion accuracy by inversion result graph, regression equation and error distribution statistical

histogram, and compares this model with other model in accuracy. The inversion SST data are compared with MODIS SST products to verify the credibility of the model. The model is applied to South China Sea SST inversion to further verify the adaptability of the inversion model in different sea areas, and this section discusses the reasons for the reduced accuracy.

5.1. Compared with measured data in accuracy

The SST inversion is carried out by the model established in this paper. The inversion results are compared with the 173 sets of measured SST data to verify the inversion accuracy. The results are plotted in Fig. 4, it shows that the inversion SST is roughly consistent with the measured SST. Most of the inversion values fluctuate slightly above and below the measured values except for few special points.

The linear regression graph of the inverted SST and the measured SST can be obtained by statistical regression, the results are shown in Fig. 5. The linear regression coefficient of the two values is 0.988, the regression equation is $y = 1.0167x - 0.0014$. In the inversion SST results, the mean absolute deviation is 0.85 °C, the standard error is 0.71 °C, and the maximum absolute error is 4.05 °C. The pie chart for the number of the error is shown in Fig. 6, the absolute error within 0.5 °C accounts for 52.87%, the absolute error within 1 °C accounts for 84.97%, and the absolute error above 1 °C accounts for 15.03% [21].

As shown in Table 4, it can be found that the model comes up in this paper has higher precision compared with other methods.

The SST inversion model based on deep learning has better overall accuracy, but there are cases where the accuracy of individual sample points has poor accuracy. The reasons for affecting the accuracy of model inversion are as follows:

(1) The model training is insufficient due to the small amount of measured data. Deep learning learns features through large amounts of data, the small amount of data may affect the accuracy of the inversion [24].
(2) The remote sensing data has not been processed to remove the cloud. Although the selected MODIS remote sensing data are clear sky data, some pixels are still covered by thin clouds, resulting in low inversion accuracy.
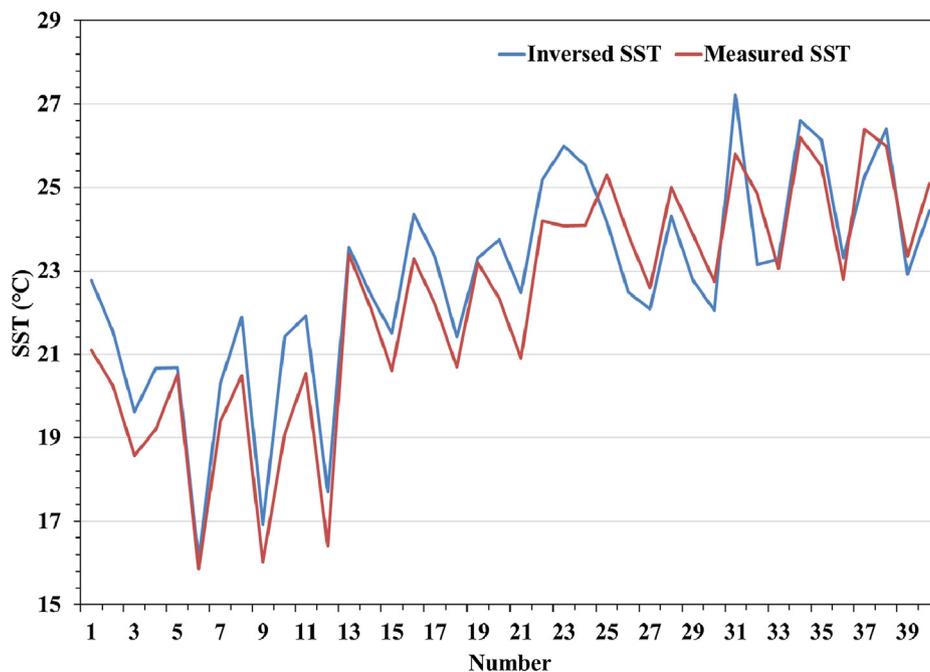

Fig. 10. Portability Analysis in South China Sea.

(3) The remote sensing data is not exactly corresponding to the measured data in time and space. The error of the measured data and the MODIS data is within ± 0.5 h in time; the buoys only collect the SST point data, but the resolution of the image inversion is 1 km, indicating the mean SST in this area.

5.2. Compared with MODIS SST products in accuracy

82 sets of inversion SST data are compared with the MODIS SST products and the measured SST data to verify the credibility of the model [25]. The specific ideas are the following steps. First, the data in Network Common Data Form (NetCDF) corresponding to the measured data in time are obtained from the PODAAC website using python module [26]. Second, the Scientific DataSet (SDS) library reads the acquired NetCDF data to get the data corresponding to the measured data in space. The MODIS SST products corresponding to the measured data in time and space are obtained by these two steps. Then, these corresponding SST inversion data are obtained from the model. Finally, three types of SST data are plotted. Fig. 7 is a comparison of measured SST data, inversion SST data, and MODIS products SST data. The mean absolute deviation of the inversion SST is 0.67 °C; the mean absolute deviation of the MODIS products SST is 0.81 °C. The model has high reliability in SST inversion by the analysis.

The original MODIS image in 2016 is randomly selected to invert the regional SST in Bohai and compare the SST with MODIS SST production. The first picture in each group is MODIS SST production, the second is the inversion result of the model, the third is the difference between them, and the fourth is the MODIS processed image. The inversion accuracy is analyzed by the MSE and the mean absolute deviation. The three sets of data error analysis are shown in the Table 5. By comparison and analysis, the reasons for the error are as follows: water vapor in places with large temperature differences [27]; clouds (circled in Fig. 8) in the MODIS image; different environment elements such as illumination in different time. These factors lead to differences in MODIS images, which affects inversion SST accuracy. In general, the overall regional SST inversion results are good and shown in Fig. 8.

5.3. Portability analysis of this model

The 40 sets of buoys in South China Sea are used to verify the applicability of the model in other sea areas. The position of the buoy is shown in Table 6 and Fig. 9. The measured SST and inversion SST in South China Sea are shown in Fig. 10. The standard error is 1.36 °C and the maximum absolute error is 3.86 °C. The distribution of absolute error is statistically calculated, the absolute error within 0.5 °C accounts for 30% in the total sample, the absolute error within 1 °C accounts for 57.5% in the total sample, and the absolute error above 1 °C accounts for 42.5% in the total sample.

Comparing the inversion results in Bohai with other sea areas, it can be found that the inversion accuracy of the model is still good when applied to other sea areas, showing the portability of the model. But the inversion accuracy of the South China Sea has decreased because the sea conditions, atmospheric water vapor content, weather conditions, temperature and other environmental factors are different in different sea areas and the training data in the inversion model are from Bohai. The model data can be trained by using data in other sea areas and fine-tuning the model parameters to improve the inversion precision in other sea areas.

6. Conclusion

This paper presents a DNN inversion SST model, which introduces the deep learning method to replace the traditional regression statistical method. The model is established by DNN with multiple hidden layers to invert the SST in Bohai. The determination coefficient of inversion and measured values is 0.98, the standard error is 0.71 °C and the mean

absolute deviation is 0.85 °C, which shows good accuracy of the model. The accuracy of Bohai SST inversion results is compared with MODIS SST products, which verifies the credibility of the model. Then the inversion model is applied to other sea areas to prove the portability of the model. The higher precision inversion results demonstrate the feasibility of applying deep learning to SST inversion.

The accuracy of individual points in the inversion results is poor since SST inversion is a complicated problem. There are still many other aspects to improve accuracy in the inversion model. In the future research, the inversion model should be further optimized by selecting reasonable remote sensing parameters and increasing the amount of training data. In addition, the corresponding sea area data can be added to inversion model to improve the adaptability in different sea areas for the case where the accuracy of the inversion model decreases in different sea areas.

Conflict of interest

None.

Appendix A. Supplementary material

Supplementary data to this article can be found online at https://doi.org/10.1016/j.infrared.2019.04.022.

References

[1] Y. Zhang, T. Zhang, Structure-guided unidirectional variation de-striping in the infrared bands of MODIS and hyperspectral images, Infrared Phys. Technol. 77 (2016) 132–143.
[2] C. Zhang, Y. Ren, Y. Cai, et al., Study on local monitoring model for SST in Taiwan strait based on MODIS data, J. Trop. Meteorol. 25 (1) (2009) 73–81.
[3] E.P. McClain, W.G. Pichel, C.C. Walton, et al., Multi-channel improvements to satellite-derived global sea surface temperatures, Adv. Space Res. 2 (6) (1982) 43–47.
[4] L. Zhu, X. Gu, Q. Wang, et al., A regional algorithm to estimate sea surface temperature in the East China Sea, Remote Sens. Technol. Appl. 23 (5) (2008) 495–499.
[5] L. Liu, J. Zhou, Using MODIS imagery to map sea surface temperature, Geospatial Inform. 4 (2) (2006) 7–9.
[6] B. Yin, W. Wang, L. Wang, Review of deep learning, J. Beijing Univ. Technol. 41 (1) (2015) 48–59.
[7] Z. Xu, Remote Sensing Inversion Models of Sea Surface Salinity Based on Machine Learning Method[D], China University of Geosciences, Beijing, China, 2016.
[8] T. Shi, Z. Zou, Z. Shi, et al., Mudflat aquaculture labeling for infrared remote sensing images via a scanning convolutional network, Infrared Phys. Technol. 94 (2018) 16–22.
[9] J. Kim, K. Kim, J. Cho, et al., Satellite-based prediction of arctic sea ice concentration using a deep neural network with multi-model ensemble, Remote Sens. 11 (1) (2019) 19.
[10] G.E. Hinton, S. Osindero, Y.W. Teh, A fast learning algorithm for deep belief nets, Neural Comput. 8 (7) (2006) 1527–1554.
[11] A.E. Orhan, W.J. Ma, Efficient probabilistic inference in generic neural networks trained with non-probabilistic feedback, Nat. Commun. 8 (1) (2017) 1–14.
[12] Y. Lecun, Y. Bengio, G. Hinton, Deep learning, Nature 521 (7553) (2015) 436.
[13] Z. Wan, New refinements and validation of the MODIS land-surface temperature/emissivity products, Remote Sens. Environ. 112 (1) (2008) 59–74.
[14] Y. Lin, The Inversion of Sea Surface Temperature Based on Multi-Source Remote Sensing—A Case Study of Yueqing Bay[D], East China Normal University, Shanghai, China, 2013.
[15] K. Mao, Z. Qin, Retrieval of water content of atmosphere in Bohai region by MODIS image, Remote Sens. 4 (2004) 47–49.
[16] X. Glorot, A. Bordes, Y. Bengio, Deep sparse rectifier networks, J. Mach. Learn. Res. 14 (2011) 315–323.
[17] A. Krizhevsky, I. Sutskever, G. Hiton, Imagenet classification with deep convolutional neural networks, Adv. Neural Inform. Process. Syst. (2012) 1097–1105.
[18] N. Srivastava, G.E. Hinton, A. Krizhevsky, Dropout: a simple way to prevent neural networks from overfitting, J. Mach. Learn. Res. 15 (1) (2014) 1929–1958.
[19] A. Swami, R. Jain, Scikit-learn: machine learning in python, J. Mach. Learn. Res. 12 (10) (2013) 2825–2830.
[20] D. Kingma, J. Ba, Adam: a method for stochastic optimization, arXiv preprint arXiv:1412.6980, 2014.
[21] J. Jin, Y. Wang, H. Jiang, X. Chen, Evaluation of microclimatic detection by a wireless sensor network in forest ecosystems, Scient. Rep. 8 (2018) 1–9.
[22] J. Song, Study on the Retrieval and Application of SST based on MODIS Data[D], Xidian University, Xian, Shanxi, China, 2011.
[23] C. Su, K. Xiao, N. Ye, Retrieval of sea surfaee temperature in Fujian coastal region by using MODIS remote sensing data, Mar. Inform. 1 (2014) 1–10.
[24] L. Breiman, Bagging predictors, Mach. Learn. 24 (2) (1996) 123–140.

[25] D. Fu, X. Xia, J. Wang, et al. Synergy of AERONET and MODIS AOD products in the estimation of PM 2.5, concentrations in Beijing, Sci Rep, 8 (1) (2018) 10174.

[26] M. Kummu, M. Taka, J.H.A. Guillaume, Gridded global datasets for gross domestic product and human development index over 1990–2015, Scient. Data 5 (2018) 180004.

[27] M. Fujita, T. Sato, Observed behaviours of precipitable water vapour and precipitation intensity in response to upper air profiles estimated from surface air temperature, Sci Rep 7 (1) (2017) 4233.